Journal of Diabetes & Metabolic Disorders (2022) 21:429–438
https://doi.org/10.1007/s40200-022-00989-2

RESEARCH ARTICLE

Ficus benghalensis promotes the glucose uptake- Evidence with *in silico* and *in vitro*

Vaishnavi Shankar Madiwalar[1] · Prarambh S. R. Dwivedi[1] · Ashwini Patil[1] · Soham M. N. Gaonkar[1] · Vrunda J. Kumbhar[1] · Pukar Khanal[1] · B. M. Patil[1]

Received: 7 September 2021 / Accepted: 23 January 2022 / Published online: 15 February 2022

Abstract

Background *Ficus benghalensis* L. is traditionally used to manage diabetes; also used in various herbal formulations, and is indicated as an insulin sensitizer. Hence, present work attempted in identifying the probable lead hits to promote glucose uptake *via* computational approach followed by experimental evaluation of hydroalcoholic extract of *Ficus benghalensis* L. bark in yeast cells.

Methods The *in vitro* assay for glucose uptake was performed in the baker yeast whereas *in-silico* study involved retrieving the phytoconstituents from open sources, and predicting for probable targets of diabetes followed by drug-likeness score, probable side effects, and ADMET profile. Homology modeling was performed to construct the target protein glucose transporter-2. In addition, the binding affinity of each ligand with glucose transporter was predicted using AutoDock 4.2.

Results A total of 17 phytoconstituents from *F. benghalensis* were identified to possess the anti-diabetic effects. Among them, 4-methoxybenzoic acid scored the highest drug-likeness score and lupeol acetate had the maximum binding affinity of -8.02 kcal/mol with 9 pi-interactions *via Tyr324, Phe323, Ile319, Ile200, Ile28, Phe24,* and *Ala451*. Similarly, the extract showed the highest glucose uptake efficacy in yeast cells at 500 µg/mL.

Conclusion Herein the present study reflected the probable activity of the phytoconstituents from *F. benghalensis* in promoting the glucose uptake *via* the *in silico* and *in vitro* approaches.

Keywords Diabetes mellitus · *Ficus benghalensis* · Glucose uptake · Glucose transporters (GLUTs) · Molecular modeling (*in-silico* studies) · *Saccharomyces cerevisiae*

Abbreviations

3D	3 Dimensional
ADMET	Absorption, distribution, metabolism, and excretion
ChEBI	Chemical Entities of Biological Interest
DM	Diabetes Mellitus
PDB	Protein data bank
RCSB	Research Collaboratory for Structural Bioinformatics
SMILES	Simplified molecular-input line-entry system

Introduction

Diabetes mellitus (DM) is polygenic pathogenesis due to disturbed carbohydrate, fat, and protein metabolism resulting from defects in insulin action or secretion or both [1, 2]. In the USA, more than 20 million populations were estimated as diabetic in 2005 and have been predicted to rise to 48 million by 2050 [3]. An under-expression of glucose transporters for a long-term period results in elevated blood glucose levels and other pathological conditions of DM [4]. Hence targeting the glucose transporters (GLUTs) may serve as a potential approach for treating this disease. The uptake of glucose follows multiple mechanisms; one such is facilitated diffusion mediated by GLUTs [5]. The uptake of

Vaishnavi Shankar Madiwalar and Prarambh S. R. Dwivedi contributed equally.

✉ Pukar Khanal
pukarkhanal58@gmail.com

✉ B. M. Patil
bmpatil59@hotmail.com; drbmpatil@klepharm.edu

[1] Department of Pharmacology and Toxicology, KLE College of Pharmacy Belagavai, KLE Academy of Higher Education and Research (KAHER), Belagavi 590010, India

glucose takes place in tissues such as skeletal muscles and the liver where cells utilize glucose for the production of energy [6, 7] involving sodium-dependent glucose co-transporters-2 (SGLT-2) and GLUT. There are 14 members in the GLUT family *i.e.* GLUT-1 to GLUT-14, in which GLUT-2 is predominant in kidney, gut, liver, pancreatic β-cells and GLUT-4 is predominant on skeletal muscles and adipose tissue [8].

Medicinal plants compose multiple secondary bio-actives with potential medicinal values [9–11]. Furthermore, indigenous medicines are preferred above synthetic oral hypoglycaemic agents due to their large margin of safety [12]. *Ficus benghalensis* L. commonly known as banyan, banyan fig, and Indian banyan, belonging to the family, Moraceae [13] is a holy large evergreen tree with aerial roots. It is also recognized for its various remarkable medicinal properties in folk and traditional system of medicine [14]. The significant benefits of the tree are known to have treatment in dysentery, diarrhea, rheumatism, skin disorders, analgesics, anti-inflammatory, anti-tumor, hypolipidaemic, and other life-threatening diseases [15]. *F. benghalensis* bark has been reported to compose flavonoids, polyphenols, steroids, and triterpenes; recognized for their antidiabetic efficacy [16]. Studies also report *F. benghalensis* to possess the anti-diabetic activity and inhibitory actions on α-amylase and α-glucosidase enzymes and have glucose uptake efficacy in isolated rat-hemidiaphragm [16, 17].

The current drug discovery employs the principle of *lock and key* for ligand-target interaction [18]. However, for polygenic conditions like diabetes, it must be understood that multiple bio-actives present in plants may act through different mechanisms by targeting multiple proteins [19, 20]. In addition, the mechanism of glucose uptake of *Saccharomyces cerevisiae* fungus is similar to that of human cells [21, 22] which utilize glucose to produce carbon dioxide, ethanol, and energy. The yeast cells consume glucose by enhancing the glucose uptake via glucose uptake transporters [23]. Herein, the present study aimed to identify the efficacy of hydro-alcoholic extract of *F. benghalensis* (FBE) to enhance the glucose uptake in yeast cells and predict the bio-active possessing the highest binding affinity with protein GLUT 2 *via in-silico* molecular docking.

Material and methods

Collection of plant and preparation of hydro-alcoholic extract

The collected plant part (bark of wild-grown *F. benghalensis* L.) was authenticated at ICMR-NITM, Belagavi; herbarium accession number *RMRC-1405*. The collected plant *F. benghalensis* (bark) was washed under running water, shade dried, and turned into a coarse powder, and FBE was prepared as detailed by Cos et al. [24].

Mining of bio-actives and their drug-likeness score

A list of reported phytoconstituents was retrieved from the ChEBI (https://www.ebi.ac.uk/chebi/) [25] and their molecular formula and weight, PubChem CID, and canonical SMILES were retrieved from the PubChem (https://pubchem.ncbi.nlm.nih.gov/) database. Further, the drug-likeness score of bioactive was predicted using "Lipinski's rule of five" model *via* MolSoft (http://www.molsoft.com/) [26].

Adverse effect and ADMET profile prediction

The probable adverse effects of each compound were predicted using the ADVERPred (http://www.way2drug.com/adverpred/) [27]. Similarly, probable cytotoxicity, absorption, metabolism, excretion, and toxicity (ADMET) profile of bio-actives were obtained using admetSAR 2.0 (http://lmmd.ecust.edu.cn/admetsar2/) [28].

Glucose uptake by yeast cells

The glucose uptake assay in yeast cells was performed as explained by Cirillo [29]. Percentage change in glucose uptake in yeast cells by FBE was determined and compared with metronidazole. The yeast cells suspension *i.e.* 1% w/v were soaked overnight followed by centrifugation (4200 rpm, 5 min); supernatant (10 mL) was added with 90 mL distilled water. Different concentrations of FBE and metronidazole were suspended in glucose solution *i.e.* 500 ng/mL and incubated (37˚C, 10 min). Later, 3,5-dinitrosalicylic acid reagent (2 mL) was added along with distilled water to make up the volume and incubated (37˚C, 60 min) and centrifuged (3800 rpm, 5 min). The absorbance was recorded at 520 nm in UV spectroscopy. Blank absorbance was also recorded; % glucose uptake was calculated as

$$\%\text{glucoseuptake} = \left(1 - \frac{As}{Ac}\right)X100$$

where "*Ac*" and "*As*" represent the absorbance of the control and test respectively.

In-silico molecular docking

Ligand preparation

3D structures of ligands were retrieved from the PubChem (https://pubchem.ncbi.nlm.nih.gov/) database in.sdf and

converted into.pdb using Discovery Studio visualizer (https://discover.3ds.com/discovery-studio-visualizer-download)2021. The energy of each ligand was minimized using the MMFF94 force field [30] and converted into a.pdbqt as a ligand molecule.

Macromolecule preparation

Homology modeling was utilized for generating the 3D structure of GLUT2 protein. FASTA sequence (ID: P11168-1) containing 524 amino acid residue was obtained from the UniProt database (https://www.uniprot.org/). The template 4zwc.1.A with 96% total query coverage and zero E-value was chosen to build the model based on GMEQ and QMEAN; achieved 0.79 and 3.42 respectively using SWISS-MODEL (https://swissmodel.expasy.org/). The protein was visualized *via* Discovery studio visualizer 2021 and the distribution of the amino acids of protein was visualized in PROCHECK (https://www.ebi.ac.uk/thornton-srv/software/PROCHECK/) [31] to allocate the amino acids in most favored, additional allowed, generously allowed, and disallowed regions in Ramachandran plot.

Ligand–protein docking

Autodock 4.2 (https://autodock.scripps.edu/) was used to dock the ligands against the target protein within a grid size X-, Y-, Z-dimension 104, 108, 110, and x-, y-, z-center -48.424, 5.411, 16.031 and genetic algorithm as search method using Cygwin terminal (https://www.cygwin.com/). The ligand pose with the lowest binding energy was chosen to visualize the ligand–protein interactions in Discovery Studio 2021.

Results

Identification of bioactive and biological spectrum

Twenty-four different phytoconstituents were identified in *F. benghalensis* from ChEBI (https://www.ebi.ac.uk/chebi/) and other open-source records. Among twenty-four molecules, seventeen were predicted to possess biological spectra with the keyword "*Diabetic*"; Table 1. Further, PubChem CID, molecular weight, and molecular formula of the respected bioactives are presented in Table 2.

Probable side effects, ADMET profile, and drug-likeness of compounds

Except for 3-*O*-*trans*-p-coumaroyltormentic acid, mucusisoflavone C, 24-methylenecycloartanol, isowighteone, lupeol acetate, wighteone, psoralen, and ursolic acid; the rest of phytoconstituents were predicted for different side effects; including cardiac failure, arrhythmia, myocardial infarction, hepatoxicity, and nephrotoxicity (Fig. 1). Also, phytoconstituents were predicted for their probability for human intestinal absorptivity, isoenzyme inhibition, blood–brain barrier permeability, plasma protein binding, and mutagenicity (Fig. 2). Similarly, all seventeen compounds were predicted for a drug-likeness score in which 4-methoxybenzoic acid was traced for the highest (Table 3) which indicated better intestinal absorbtivity compared to other secondary metabolites.

Homology modeling of GLUT2 and molecular docking

Ramachandran plot analysis of the homology modeled protein revealed 91.6% of the total amino acid residues to be distributed in the most favorable, 7.4% in the additional allowed, 0.7% in the generously allowed, and 0.2% in the disallowed regions (Fig. 3).

Among all the bioactive, lupeol acetate was observed to possess the highest binding affinity (binding energy -8.02 kcal/mol, IC_{50} 1.32 µM) with GLUT-2. Although no hydrogen bond interaction was observed within the ligand-GLUT-2 complex, 9 pi interactions were observed with 7 amino acid residues *i.e. Tyr324*, *Phe323*, *Ile319*, *Ile200*, *Ile28*, *Phe24*, and *Ala451* (Table 4). The ligand–protein interaction of top 5 lead hits *i.e.* lupeol acetate, isoderrone, *24*-methylenecycloartanol, isoweighteone, and weighteone against GLUT2 is presented in Fig. 4.

In vitro glucose uptake assay in yeast cells

The highest glucose uptake was high if exposed to 500 µg/mL of FBE (log concentration ~ 2.7 µg/mL). Also, the glucose uptake was observed to be directly proportional to the concentration of FBE. In contrast, the highest glucose uptake was within the lowest concentration *i.e.* 62.5 µg/mL (log concentration ~ 1.8 µg/mL) of metronidazole (Fig. 5).

Discussion

An anabolic hormone, insulin; produced by the pancreatic β-cells regulates the blood glucose level by promoting glucose uptake on adipose tissue and skeletal muscles [32]. An endocrine disorder, diabetes occurs due to insulin deficiency which is characterized by uncontrolled postprandial and fasting hyperglycemia; severe form is reflected by protein wasting and ketosis [33]. Literature reflects that anti-hyperglycemic agents may act by either one or more mechanisms

Table 1 Biological spectra of secondary metabolites from *F. benghalensis*

Phytoconstituents	Pa	Pi	Anti-diabetic spectra
3-O-trans-p-coumaroyltormentic acid	0.285	0.091	Antidiabetic
benjaminamide	0.23	0.038	Diabetic nephropathy treatment
mucusisoflavone C	0.203	0.121	Antidiabetic symptomatic
isoderrone	0.207	0.117	Antidiabetic symptomatic
isowighteone	0.225	0.136	Diabetic retinopathy treatment
	0.286	0.048	Antidiabetic symptomatic
apigenin	0.225	0.136	Antidiabetic
	0.32	0.029	Antidiabetic symptomatic
	0.181	0.025	Antidiabetic (type 1)
lupeol acetate	0.352	0.106	Diabetic neuropathy treatment
3',4',5,7-tetrahydroxy-3-methoxyflavone	0.35	0.02	Antidiabetic symptomatic
4-methoxybenzoic acid	0.152	0.051	Antidiabetic (type 1)
	0.238	0.046	Antidiabetic (type 2)
	0.343	0.022	Antidiabetic symptomatic
	0.364	0.054	Antidiabetic
	0.372	0.075	Diabetic neuropathy treatment
	0.295	0.007	Diabetic nephropathy treatment
	0.209	0.012	Diabetic retinopathy treatment
kaempferol	0.372	0.016	Antidiabetic symptomatic
	0.202	0.016	Antidiabetic (type 1)
	0.196	0.169	Antidiabetic
3,4-dihydroxybenzoic acid	0.373	0.051	Antidiabetic
	0.341	0.022	Antidiabetic symptomatic
	0.285	0.008	Diabetic nephropathy treatment
	0.374	0.072	Diabetic neuropathy treatment
	0.269	0.037	Antidiabetic (type 2)
	0.186	0.023	Antidiabetic (type 1)
	0.179	0.025	Diabetic retinopathy treatment
asperphenamate	0.157	0.044	Antidiabetic (type 1)
	0.286	0.247	Diabetic neuropathy treatment
24-methylenecycloartanol	0.389	0.053	Diabetic neuropathy treatment
wighteone	0.251	0.075	Antidiabetic symptomatic
psoralen	0.152	0.05	Antidiabetic (type 1)
daucosterol	0.299	0.083	Antidiabetic
	0.299	0.217	Diabetic neuropathy treatment
ursolic acid	0.451	0.014	Antidiabetic (type 2)
	0.417	0.039	Antidiabetic

Pa**:** Pharmacological activity, ***Pi*****:** Pharmacological inactivity**,**

Low **High**

Table 2 Secondary metabolites from *F. benghalensis* along with their PubChem CID, molecular weight, and formula

Phytoconstituents	PubChem CID	Molecular weight	Molecular formula
3-O-trans-p-coumaroyltormentic acid	14,335,955	634.39	$C_{39}H_{54}O_7$
benjaminamide	56,662,789	681.63	$C_{42}H_{83}NO_5$
mucusisoflavone C	53,344,647	674.22	$C_{40}H_{34}O_{10}$
isoderrone	14,237,660	336.1	$C_{20}H_{16}O_5$
isowighteone	5,494,866	338.12	$C_{20}H_{18}O_5$
apigenin	5,280,443	270.05	$C_{15}H_{10}O_5$
lupeol acetate	92,157	468.4	$C_{32}H_{52}O_2$
3',4',5,7-tetrahydroxy-3-methoxyflavone	5,280,681	318.06	$C_{16}H_{12}O_7$
4-methoxybenzoic acid	7478	152.05	$C_8H_8O_3$
kaempferol	5,280,863	286.05	$C_{15}H_{10}O_6$
3,4-dihydroxybenzoic acid	72	154.03	$C_7H_6O_4$
asperphenamate	173,952	506.22	$C_{32}H_{30}N_2O_4$
24-methylenecycloartanol	94,204	440.4	$C_{31}H_{52}O$
wighteone	5,281,814	338.12	$C_{20}H_{18}O_5$
psoralen	6199	186.03	$C_{11}H_6O_3$
daucosterol	5,742,590	576.44	$C_{35}H_{60}O_6$
ursolic acid	64,945	456.36	$C_{30}H_{48}O_3$

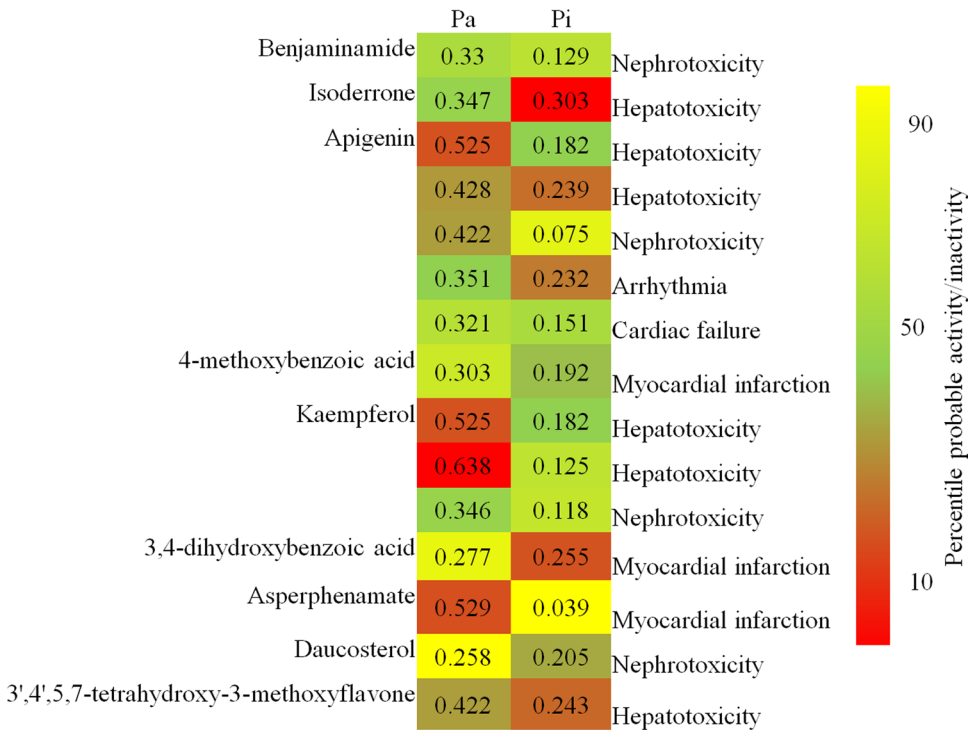

Fig. 1 Probable side effects of bioactives from *F. benghalensis*, *Pa*: Probable activity, ***Pi*:** Probable inactivity

i.e. increasing the insulin secretion, restoring the pancreatic β-cells, favoring glucose utilization, and obstructing the activity of the hydrolyzing enzyme *i.e.* α-amylase and α-glucosidase [34] and the glucose transporters [35].

In ancient literature (*Ayurveda*), diabetes is linked with four different disease conditions depending upon the clinical features; including "*sthaulya*", "*kaphaja prameha*", "*pittaja prameha*", *or* "*madhumeha*" [36]. The phytoconstituents from *F. benghalensis* are reported to enhance glucose transport and promote its catabolism into the muscle or stimulate insulin secretion. Since the glucose transport is concentration-dependent, it has been noted that glucose

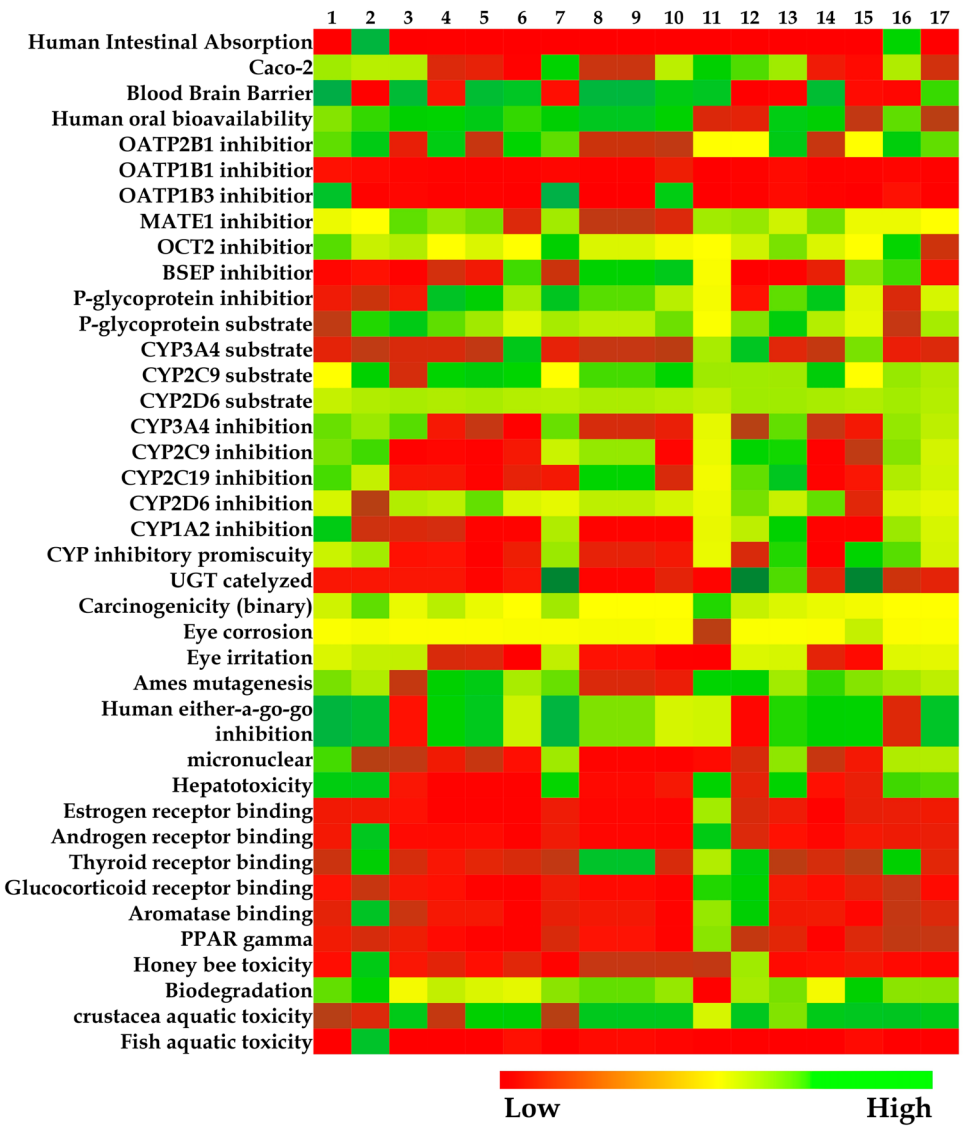

Fig. 2 ADMET profile of reported bioactives *i.e.* (*1*) 3-*O*-*trans*-*p*-coumaroyltormentic acid, (*2*) benjaminamide, (*3*) Mucusisoflavone C, (*4*) isoderrone, (*5*) isowighteone, (*6*) apigenin, (*7*) lupeol acetate, (*8*) 3',4',5,7-tetrahydroxy-3-methoxyflavone, (*9*) 4-methoxybenzoic acid, (*10*) kaempferol, (*11*) 3,4-dihydroxybenzoic acid, (*12*) asperphenamate, (*13*) 24-methylenecycloartanol, (*14*) wighteone, (*15*) psoralen, (*16*) daucosterol, and (*17*) ursolic acid from *F. benghalensis*

transport in the adipose tissue is very low in absence of insulin and rapidly stimulated in presence of insulin [37]. The bidirectional movement of glucose across the cell membrane by facilitated glucose transporters proceeds exterior to the interior membrane of the cell particularly in metabolic active insulin-sensitive tissues [5]. Deficiency of the secondary active sodium/glucose transporters results in glucose and galactose malabsorption and congenital renal glycosuria [38, 39]. Since GLUT2 exhibits glucose transport in the gut, liver, and pancreatic islets [40, 41]; the transporter drives special attention target selection in the present study due to the higher affinity of *F. benghalensis* towards GLUT2.

Further, results from molecular docking have revealed that lupeol acetate possessed the highest binding affinity with GLUT-2 indicating the potential of lupeol as anti-diabetic. Similarly, Reddy et al. reported lupeol to possess anti-diabetic potential on streptozotocin-induced hyperglycemia in rats which may be due to the property of lupeol to potentiate glucose uptake *via* GLUT2[42]. Moreover, a study conducted by Satnarayana et al. revealed the potential of lupeol as an anti-diabetic agent acting through insulin receptors and GLUT [43]. Similarly, a study conducted by Shreenithi et al. reported the potency of lupeol as antidiabetic; revealed that it significantly reduced hyperinsulinemia in sucrose-induced rats, which may be *via* the regulation of insulin receptor and GLUT expression in gracilis muscle [44]. Also, in the previous study, lupeol has been reported to form hydrogen bond interactions with *Val85* and *Val89*, followed by unfavorable contacts with *Asn304* with GLUT2. In addition, it had six pi-alkyl interactions with

Table 3 Druglikeness score of phytoconstituents from *F. benghalensis*

Phytoconstituents	Molecular formula	Molecular weight (g/mol)	NHBA	NHBD	MolLogP	DLS
3-O-trans-p-coumaroyltormentic acid	$C_{39}H_{54}O_7$	634.39	7	4	6.88	1.03
benjaminamide	$C_{42}H_{83}NO_5$	681.63	6	5	14.58	-0.97
mucusisoflavone C	$C_{40}H_{34}O_{10}$	674.22	10	6	7.64	0.86
isoderrone	$C_{20}H_{16}O_5$	336.1	5	2	3.52	-0.04
isowighteone	$C_{20}H_{18}O_5$	338.12	5	3	3.93	0.67
apigenin	$C_{15}H_{10}O_5$	270.05	5	3	3.22	0.39
lupeol acetate	$C_{32}H_{52}O_2$	468.4	2	0	8.49	0.2
3',4',5,7-tetrahydroxy-3-methoxyflavone	$C_{16}H_{14}O_7$	318.06	7	4	1.62	0.93
4-methoxybenzoic acid	$C_8H_8O_3$	152.05	3	1	1.95	1.3
kaempferol	$C_{15}H_{10}O_6$	286.05	6	4	1.61	0.5
3,4-dihydroxybenzoic acid	$C_7H_6O_4$	154.03	4	3	1.05	0.23
asperphenamate	$C_{32}H_{30}N_2O_4$	506.22	6	2	6.16	0
24-methylenecycloartanol	$C_{31}H_{52}O$	440.4	1	1	8.49	-0.48
wighteone	$C_{20}H_{18}O_5$	338.12	5	3	-4.36	1.06
psoralen	$C_{11}H_6O_3$	186.03	3	0	1.88	-1.13
daucosterol	$C_{35}H_{60}O_6$	576.44	6	4	5.96	0.5
ursolic acid	$C_{30}H_{48}O_3$	456.36	3	2	6.2	0.66

Low **High,** ***NHBD*****:** Number of hydrogen bond donors, ***NHBA*****:** Number of hydrogen bond acceptor, ***DLS*****:** Drug likeness score

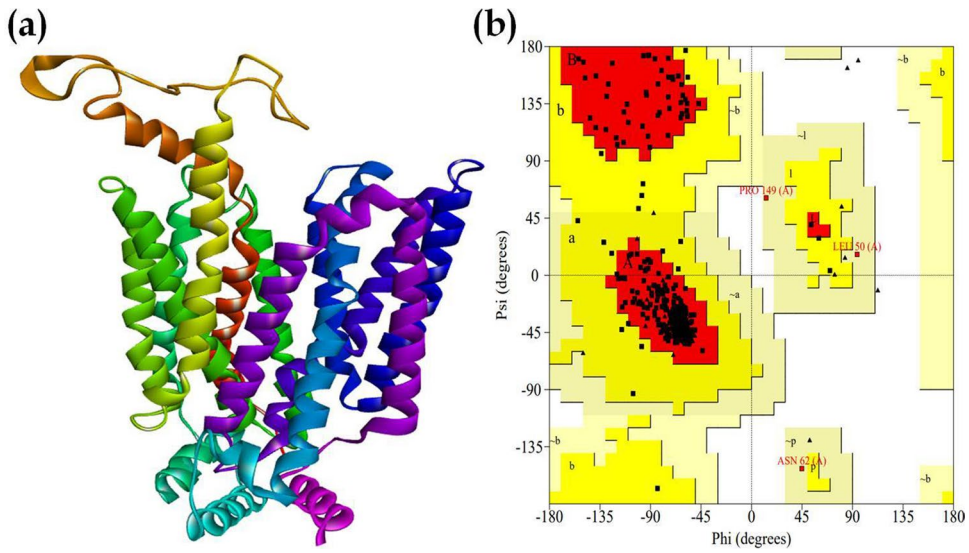

Fig. 3 (a) 3D and (b) Ramachandran plot of amino acid φ and ψ distribution of GLUT 2

Table 4 Binding affinity and interactions of phytoconstituents with GLUT2

Phytoconstituents	BE	IC_{50}	NHBI	HBR	NπB	πBR
3-O-trans-p-coumaroyltormentic acid	-5.83	53.65 µM	2	Ala475, Val465	1	Phe469
Mucusisoflavone C	-5.51	91.56 µM	3	Trp117, Ile291, Ilea438	2	Trp117, Phe441
Isoderrone	-7.4	3.75 µM	2	Gln193, Asn447	5	Ile319, Ala451, Phe454, Tyr324
Isowighteone	-7.1	6.21 µM	3	Thr69, Asp51, Ser63	2	Pro68
Apigenin	-6.19	29.07 µM	4	Thr24, Ser63, Asp52, Thr69	2	Arg53
Lupeol acetate	-8.02	1.32 µM	0	0	9	Tyr324, Phe323, Ile319, Ile200, Ile28, Phe24, Ala451
3',4',5,7-tetrahydroxy-3-methoxyflavone	-6.03	37.77 µM	2	Asn62, Thr69	1	Ilea28
4-methoxybenzoic acid	-3.9	1.38 mM	3	Lys502, Phe482, Lys483	1	Pro485
Kaempferol	-5.54	86.7 µM	3	Asn62, Thr69	2	Asp52
3,4-dihydroxybenzoic acid	-3.9	1.38 mM	5	Ile291, Trp117, Phe113, Gly16	1	Phe113
Asperphenamate	-5.32	126.96 µM	0	0	1	Phe323
24-methylenecycloartanol	-7.32	4.29 µM	1	Val109	7	Tyr324, Ala451, Ala105, Val101, Ile28, Phe323
Wighteone	-6.59	14.87	2	Asp51, Thr69	1	Arg53
Psoralen	-5.49	94.86 µM	0	0	2	Phe24, Trp444
Daucosterol	-5.89	133.37	3	Lys337, Ser336	5	Met401, Phe405, Ile402, Ile335, Ala341
Ursolic acid	-5.83	8.24 µM	3	Lys255, Arg262, Phe238	5	Pro240, Leu250

BE**:** Binding energy (kcal mol^{-1}), ***IC*****:** Inhibitory concentration, ***NHBI*****:** Number of hydrogen bond interactions, ***HBR*****:** Hydrogen bond residues, NπB**:** Number of π bonds, ***πBR*****:** π bond residues

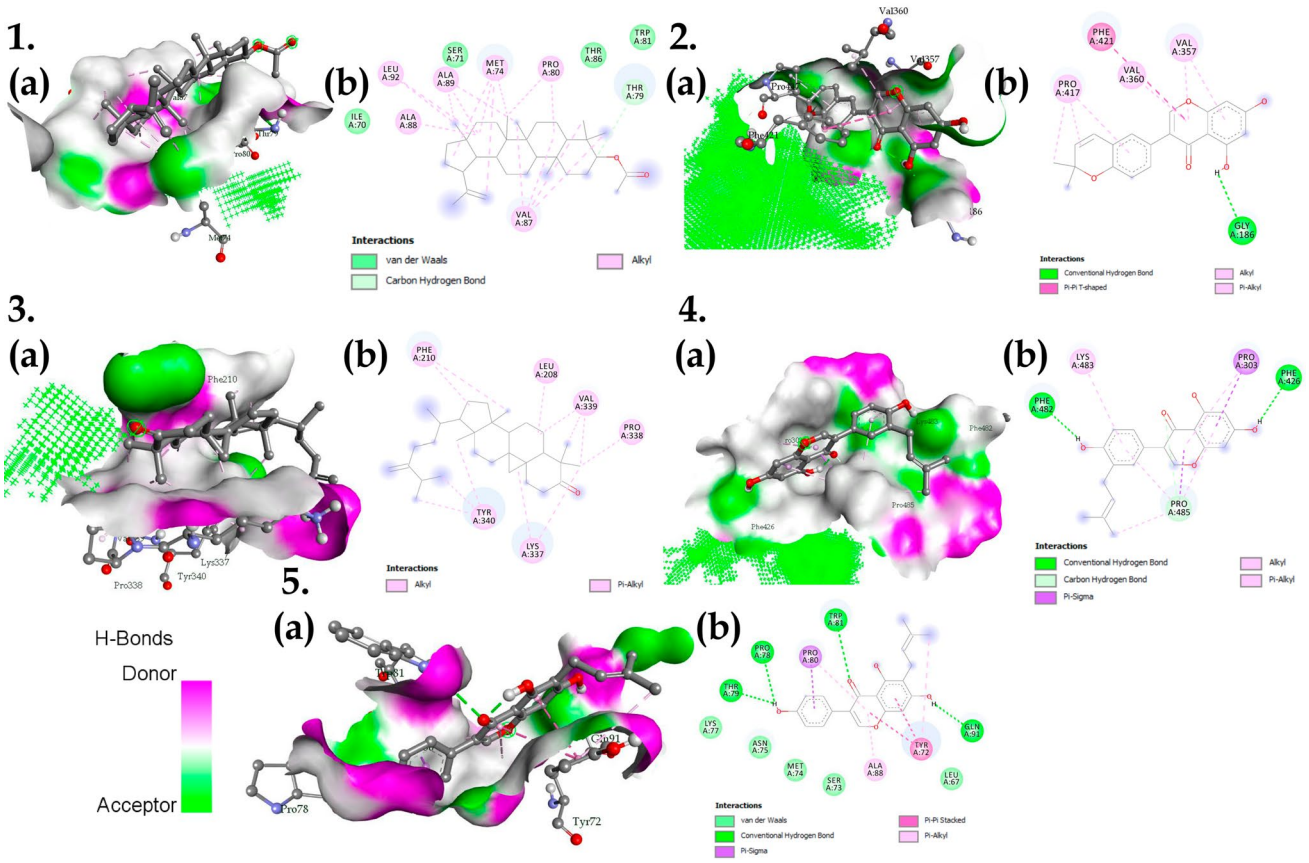

Fig. 4: 2D and 3D interaction of (1) lupeol acetate, (2) isoderrone, (c) 24-methylenecycloartanol, (4) isoweighteone, (5) weighteone with GLUT 2

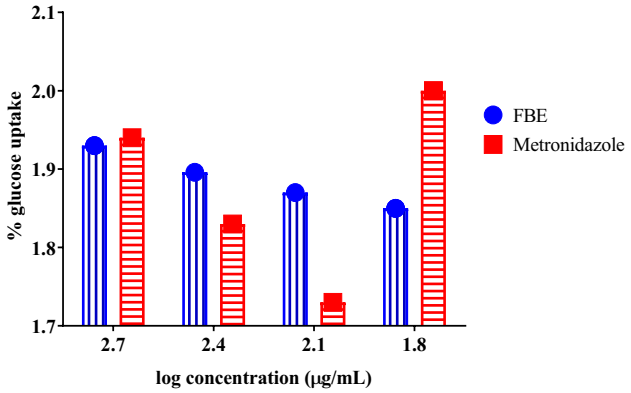

Fig. 5 Effect of FBE on glucose uptake in yeast cells

Ile42, *Ile180*, *Ile184*, *Phe307*, *Phe395*, and *Tyr308* [45]. However, in the present study, lupeol acetate had nine pi-alkyl interactions *i.e. Tyr324*, *Phe323*, *Ile319*, *Ile200*, *Ile28*, *Phe24*, and *Ala451* however, had no hydrogen bond interactions. In addition, no unfavorable interactions were formed by lupeol acetate with GLUT.

It is been reported that the glucose transport in the cell membrane is mediated by a specific membrane carrier that follows a facilitated diffusion process [4]. An effective transport down the concentration gradient occurs if intracellular glucose is adequately reduced [3]. Hence this principle can be correlated with the glucose transport mechanism. Since the pathogenesis of hyperglycemia comprises highly attenuated glucose transporters [46], our present study suggests the efficacy of FBE to enhance the glucose uptake.

Conclusion

Herein, we screened the FBE for its glucose uptake efficacy in yeast cells. Also, we docked the reported bioactives from *F. benghalensis* against GLUT. However, this data needs to be further validated via the isolation of individual bioactive and assess its glucose uptake efficacy by incubating the yeast along with the test agent in the presence of glucose. Since FBE contributed to glucose utilization, it may also involve in glucose homeostasis. Also, the molecular docking data needs to be further validated using molecular dynamics simulations which are one of the prospects of the present work.

Acknowledgements The authors are thankful to Principal KLE College of Pharmacy Belagavi, KLE Academy of Higher Education and Research (KAHER) Belagavi.

Funding This work has not received any funds from any national or international agencies in any financial or non-financial means to declare.

Declarations

Conflict of interest All the authors of this manuscript declare that they do not have any conflict of interest in any financial means. All the authors have read and approved this manuscript.

Ethical statement This work does not include any animal or human participation.

References

1. LeRoith D. β-cell dysfunction and insulin resistance in type 2 diabetes: role of metabolic and genetic abnormalities. Am J Med. 2002;113(6):3–11.
2. Ternikar SG, Patil MB, Pasha I, Dwivedi PSR. Gene ontology enrichment analysis of PPAR-γ modulators from *Cassia glauca* in diabetes mellitus. J Diabetes Metab Disord. 2021;20(2):1239–46.
3. Deshpande AD, Harris-Hayes M, Schootman M. Epidemiology of diabetes and diabetes-related complications. Phys Ther. 2008;88(11):1254–64.
4. Vargas E, Podder V, Carrillo Sepulveda MA. Physiology, Glucose Transporter Type 4. [Updated 2021 May 9]. In: StatPearls [Internet]. Treasure Island (FL): StatPearls Publishing; 2021. Available from: https://www.ncbi.nlm.nih.gov/books/NBK537322/
5. Navale AM, Paranjape AN. Glucose transporters: physiological and pathological roles. Biophys Rev. 2016;8(1):5–9.
6. El Bacha T, Luz M, Da Poian A. Dynamic Adaptation of Nutrient Utilization in Humans. Nat Educ. 2010;3(9):8.
7. Chadt A, Al-Hasani H. Glucose transporters in adipose tissue, liver, and skeletal muscle in metabolic health and disease. Pflugers Arch. 2020;472(9):1273–98.
8. Mueckler M, Thorens B. The SLC2 (GLUT) family of membrane transporters. Mol Aspects Med. 2013;34(2–3):121–38.
9. Sofowora A, Ogunbodede E, Onayade A. The role and place of medicinal plants in the strategies for disease prevention. Afr J Tradit Complement Altern Med. 2013;10(5):210–29.
10. Dwivedi PSR, Rasal VP. Identification of PTPN1B inhibitors from *Momordica charantia* and their enrichment analysis. J Phytopharmacol. 2020;9(1):38–45.
11. Dwivedi PS, Patil R, Khanal P, Gurav NS, Murade VD, Hase DP, Kalaskar MG, Ayyanar M, Chikhale RV, Gurav SS. Exploring the therapeutic mechanisms of *Cassia glauca* in diabetes mellitus through network pharmacology, molecular docking and molecular dynamics. RSC Adv. 2021;11(62):39362–75.
12. Duyu T, Khatib NA, Khanal P, Patil BM, Hullatti KK. Network pharmacology-based prediction and experimental validation of *Mimosa pudica* for Alzheimer's disease. J Phytopharmacol. 2020;9(1):46–53.
13. Khanal P, Patil BM. Consolidation of network and experimental pharmacology to divulge the antidiabetic action of *Ficus benghalensis* L. bark. 3 Biotech. 2021;11(5):238.
14. Khanal P, Patil BM. *In vitro* and *in silico* anti-oxidant, cytotoxicity and biological activities of *Ficus benghalensis* and *Duranta repens*. Chin Herb Med. 2020;12(4):406–13.
15. Khanal P, Patil BM. Reversal of insulin resistance by *Ficus benghalensis* bark in fructose-induced insulin-resistant rats. J Ethnopharmacol. 2022;284:114761.
16. Khanal P, Patil BM. Gene set enrichment analysis of alpha-glucosidase inhibitors from *Ficus benghalensis*. Asian Pac J Trop Biomed. 2019;9(6):263–70.
17. Khanal P, Patil BM. Integration of *in silico*, *in vitro* and *ex vivo* pharmacology to decode the anti-diabetic action

of *Ficus benghalensis* L. bark. J Diabetes Metab Disord. 2020;19(2):1325–37.
18. Dwivedi PSR, Patil VS, Khanal P, Bhandare VV, Gurav S, Harish DR, Patil BM, Roy S. System biology-based investigation of Silymarin to trace hepatoprotective effect. Comput Biol Med. 2022;142:105223.
19. Dwivedi PSR, Khanal P, Gaonkar VP, Rasal VP, Patil BM. Identification of PTP1B regulators from *Cymbopogon citratus* and its enrichment analysis for diabetes mellitus. In Silico Pharmacol. 2021;9:30.
20. Dwivedi PSR, Rasal VP, Kotharkar E, Khanal P. Gene set enrichment analysis of PPAR-γ regulators from *Murraya odorata* Blanco. J Diabetes Metab Disord. 2021;20(1):369–75.
21. Roy A, Dement AD, Cho KH, Kim JH. Assessing glucose uptake through the yeast hexose transporter 1 (Hxt1). PLoS One. 2015;10(3):e0121985.
22. Singh V, Bedi GK, Shri R. *In vitro* and *In vivo* antidiabetic evaluation of selected culinary-medicinal mushrooms (Agaricomycetes). Int J Med Mushrooms. 2017;19(1):17–25.
23. Rehman G, Hamayun M, Iqbal A, Ul Islam S, Arshad S, Zaman K, Ahmad A, Shehzad A, Hussain A, Lee I. *In Vitro* Antidiabetic Effects and Antioxidant Potential of Cassia nemophila Pods. Biomed Res Int. 2018;2018:1824790.
24. Cos P, Vlietinck AJ, Berghe DV, Maes L. Anti-infective potential of natural products: how to develop a stronger *in vitro* 'proof-ofconcept.' J Ethnopharmacol. 2006;106(3):290–302.
25. Degtyarenko K, De Matos P, Ennis M, Hastings J, Zbinden M, McNaught A, Alcántara R, Darsow M, Guedj M, Ashburner M. ChEBI: a database and ontology for chemical entities of biological interest. Nucleic Acids Res. 2007;36(s1):D344–50.
26. MolSoft molecules in silico. Drug-Likeness and molecular property prediction. Available at: https://molsoft.com/mprop/
27. Ivanov SM, Lagunin AA, Rudik AV, Filimonov DA, Poroikov VV. ADVERPred–Web service for prediction of adverse effects of drugs. J Chem Inf Model. 2018;58(1):8–11.
28. Yang H, Lou C, Sun L, Li J, Cai Y, Wang Z, Li W, Liu G, Tang Y. admetSAR 2.0: web-service for prediction and optimization of chemical ADMET properties. Bioinformatics. 2019;35(6):1067–9.
29. Cirillo VP. Mechanism of glucose transport across the yeast cell membrane. J Bacteriol. 1962;84(3):485–91.
30. Halgren TA. Merck molecular force field. I. Basis, form, scope, parameterization, and performance of MMFF94. J. Comput. Chem. 1996;17(5-6):490–519.
31. Laskowski RA, MacArthur MW, Moss DS, Thornton JM. PROCHECK: a program to check the stereochemical quality of protein structures. J Appl Crystallogr. 1993;26(2):283–91.
32. Dimitriadis G, Mitrou P, Lambadiari V, Maratou E, Raptis SA. Insulin effects in muscle and adipose tissue. Diabetes Res Clin Pract. 2011;93(S1):S52–9.
33. American Diabetes Association. Diagnosis and classification of diabetes mellitus. Diabetes Care. 2009;32(S1):S62–7.
34. Galicia-Garcia U, Benito-Vicente A, Jebari S, Larrea-Sebal A, Siddiqi H, Uribe KB, Ostolaza H, Martín C. Pathophysiology of Type 2 Diabetes Mellitus. Int J Mol Sci. 2020;21(17):6275.
35. Vallon V, Sharma K. Sodium-glucose transport: role in diabetes mellitus and potential clinical implications. Curr Opin Nephrol Hypertens. 2010;19(5):425–31.
36. Sharma H, Chandola HM. Prameha in Ayurveda: correlation with obesity, metabolic syndrome, and diabetes mellitus. Part 1-etiology, classification, and pathogenesis. J Altern Complement Med. 2011;17(6):491–6.
37. Sørensen SS, Christensen F, Clausen T. The relationship between the transport of glucose and cations across cell membranes in isolated tissues. X. Effect of glucose transport stimuli on the efflux of isotopically labelled calcium and 3-O-methylglucose from soleus muscles and epididymal fat pads of the rat. Biochim Biophys Acta. 1980;602(2):433–45.
38. Calado J, Santer R, Rueff J. Effect of kidney disease on glucose handling (including genetic defects). Kidney Int Suppl. 2011;120:S7-13.
39. Santer R, Schneppenheim R, Suter D, Schaub J, Steinmann B. Fanconi-Bickel syndrome–the original patient and his natural history, historical steps leading to the primary defect, and a review of the literature. Eur J Pediatr. 1998;157(10):783–97.
40. Thorens B. GLUT2, glucose sensing and glucose homeostasis. Diabetologia. 2015;58(2):221–32.
41. Berger C, Zdzieblo D. Glucose transporters in pancreatic islets. Pflugers Arch. 2020;472(9):1249–72.
42. Reddy KP, Singh A, et al. Synthesis of novel triterpenoid (lupeol) derivatives and their *in vivo* antihyperglycemic and antidyslipidemic activity. Bioorganic Med Chem Lett. 2009;19(15):4463–6.
43. Kottireddy S, Koora S. Lupeol exerts its antidiabetic activity through insulin receptor and glucose transporter-4 in gracilis muscle in high fat and sucrose-induced diabetic rats. Drug Invent Today. 2019;11(9):2258–64.
44. Shreenithi S, Vishnupriya V, Ponnulakshmi R, Gayathri R, Madhan K, Shyamaladevi B, Selvaraj J. In silico and in vivo approach to identify the antidiabetic activity of lupeol. Drug Invent Today. 2019;11(5):1113–6.
45. Oyinloye BE, Adekiya TA, Aruleba RT, Ojo OA, Ajiboye BO. Structure-Based Docking Studies of GLUT4 towards Exploring Selected Phytochemicals from *Solanum xanthocarpum* as a Therapeutic Target for the Treatment of Cancer. Curr Drug Discov Technol. 2019;16(4):406–16.
46. Cersosimo E, Triplitt C, Solis-Herrera C, et al. Pathogenesis of Type 2 Diabetes Mellitus. [Updated 2018 Feb 27]. In: Feingold KR, Anawalt B, Boyce A, et al., editors. Endotext [Internet]. South Dartmouth (MA): MDText.com, Inc.; 2000-. Available from: https://www.ncbi.nlm.nih.gov/books/NBK279115/